Air-Flow Field of the Melt-Blowing Slot Die via Numerical Simulation and Multiobjective Genetic Algorithms

Y. F. Sun, B. W. Liu, X. H. Wang, Y. C. Zeng

College of Textiles, Donghua University, Songjiang, Shanghai 201620, People's Republic of China

Received 28 April 2010; accepted 28 April 2010
DOI 10.1002/app.34760
Published online 9 August 2011 in Wiley Online Library (wileyonlinelibrary.com).

ABSTRACT: The air-flow field in melt blowing plays a key role in fiber drawing and nonwoven web performance. A multiobjective optimization using genetic algorithms was proposed to obtain optimum air-flow field with the lowest velocity decay and temperature decay of the air-flow field of a melt-blowing slot die. Four main geometry parameters, including slot width, head width, slot angle, and setback, were studied. The optimal results were achieved in the 50th generation with 20 individuals of each generation. The results also show that a smaller slot angle and larger slot width resulted in a lower air velocity decay and temperature decay.
 J Appl Polym Sci 122: 3520–3527, 2011

Key words: drawing; extrusion; fibers; melt; simulations

INTRODUCTION

Melt blowing is a single-step process to produce microfibers. A polymer melt is extruded from the die into two jets of hot air, which rapidly attenuate the molten polymer into microfibers. The fibers are collected as nonwoven webs directly. Nonwoven fibers find applications in an increasing number of fields, such as filtration, absorbency, hygiene, and apparel. Many significant efforts have been made to better understand the technology and to improve the equipment by researchers and engineers around the world.

The air-flow field plays a key role in the fiber formation process of melt blowing. Several researchers have studied air-flow fields by experimental methods and numerical simulations. Researchers[1–5] have measured the velocity and temperature fields during single-hole melt blowing using a Pitot tube and a thermocouple. Bresee and Ko[6] presented experimental measurements to provide air velocity and temperature information for a commercial melt-blowing machine. In recent years, numerical simulation have been developed to study the air-flow fields of melt-blowing dies. Krutka and Shambaugh[7] studied the air-flow field of the slot die by numerical simulation, and they obtained considerable agreement between the simulation results and the experimental data. Unfortunately, the air velocities that they used (the greatest was 34.6 m/s) during simulation were much smaller than those in commercial melt-blowing processes, which are usually over 250 m/s. Moreover, the air in their simulation was considered as incompressible, which is not suitable under the conditions of a mach number greater than 0.3. Moore and Shambaugh[8] considered compressibility of the air in their simulation; however, the simulation was under isothermal conditions, and the temperature decay of the air was not considered. Krutka et al.[9,10] used numerical simulation to analyze the velocity and temperature fields of six die geometries from multiple jets in a Schwarz melt-blowing die. They found that the velocity and temperature decay were affected by the die geometry significantly. Recently, we[11] simulated the air velocity and temperature fields of a melt-blowing slot die and analyzed the effects of the slot angle, slot width, and nose piece on the air-flow field.

Unlike conventional melt spinning, the air jet used in the melt-blowing process not only provides a substantial forwarding force but also has a function of preventing polymer solidification. As the polymer exits the melt-blowing die, the velocity of the air causes momentum transfer to the fiber, which results in rapid attenuation of the polymer. Concurrently, the high temperature of the air keeps the

Correspondence to: Y. C. Zeng (yongchun@dhu.edu.cn).
Contract grant sponsor: National Natural Science Foundation of China; contract grant number: 10972052.
Contract grant sponsor: Foundation for the Author of National Excellent Doctoral Dissertation of the People's Republic of China; contract grant number: 2007B54.
Contract grant sponsor: New Century Excellent Talents Plan of Chinese Ministry; contract grant number: NCET-09-0285.
Contract grant sponsor: Shanghai Dawning Program; contract grant number: 10SG33.

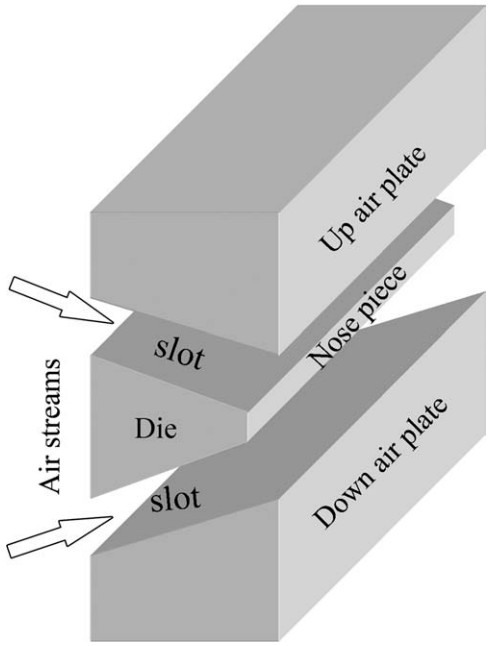

Figure 1 3D model of the slot die.

polymer at a high temperature, which aids attenuation by keeping the polymer viscosity low. The air velocity and air temperature are two key factors that affect the air-flow field of a melt-blowing die. In this study, we focus on the optimization of the geometry parameters of a melt-blowing slot die to obtain the air-flow field with optimum performance. We used a combination of numerical simulation and a genetic algorithm (GA) method to accomplish the optimization. The air velocity and temperature fields were simulated numerically; then, a multiobjective optimization was carried out with GA on the basis of the simulated results.

NUMERICAL SIMULATION AND EXPERIMENTAL VERIFICATION

Numerical simulation

There are different die geometries that are used to produce melt-blown fibers, and the slot die is one of the most commonly used dies. Figure 1 shows the three-dimensional (3D) model of a slot die. The calculation domain of the air-flow field was developed on the basis of the experiments, which is discussed later. Figure 2(a,b) shows the configuration parameters, the computational domain, and the boundary conditions. The computational domain below the die was 100 × 15 × 6 mm^3. The computational domain occupied a quarter of the total air-flow field, which was symmetric about the symmetry plane. With the help of boundary conditions of symmetry, we saved much calculation time.

In this research, we obtained the air-flow field by solving the Navier–Stokes equations through the commercial software FLUENT 6.3 (ANSYS, Canonsburg, PA):

$$\mathrm{div}(\rho\mathbf{u}) = 0 \tag{1}$$

$$\mathrm{div}(\rho u\mathbf{u}) = -\frac{\partial p}{\partial x} + \frac{\partial \tau_{xx}}{\partial x} + \frac{\partial \tau_{yx}}{\partial y} + \frac{\partial \tau_{zx}}{\partial z} + F_x \tag{2a}$$

$$\mathrm{div}(\rho v\mathbf{u}) = -\frac{\partial p}{\partial y} + \frac{\partial \tau_{xy}}{\partial x} + \frac{\partial \tau_{yy}}{\partial y} + \frac{\partial \tau_{zy}}{\partial z} + F_y \tag{2b}$$

$$\mathrm{div}(\rho w\mathbf{u}) = -\frac{\partial p}{\partial z} + \frac{\partial \tau_{xz}}{\partial x} + \frac{\partial \tau_{yx}}{\partial y} + \frac{\partial \tau_{zz}}{\partial z} + F_z \tag{2c}$$

$$\mathrm{div}(\rho\mathbf{u}T) = \mathrm{div}\left(\frac{k}{c_p}\mathrm{grad}(T)\right) + S_T \tag{3}$$

Equations (1)–(3) express the mass conservation, momentum conservation, and energy conservation of an air jet, where div is the operator of divergence,

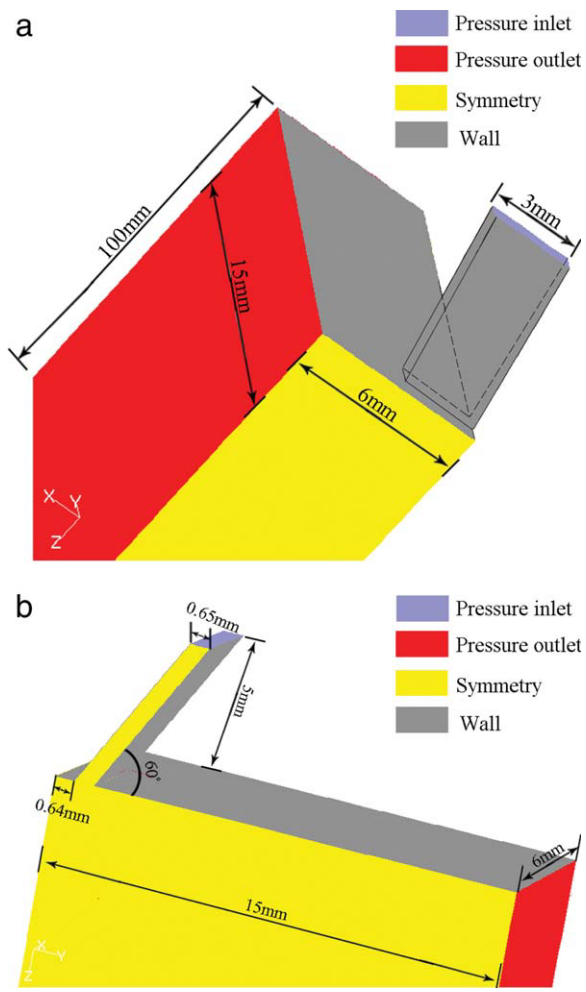

Figure 2 (a,b) Computational domain and boundary conditions. [Color figure can be viewed in the online issue, which is available at wileyonlinelibrary.com.]

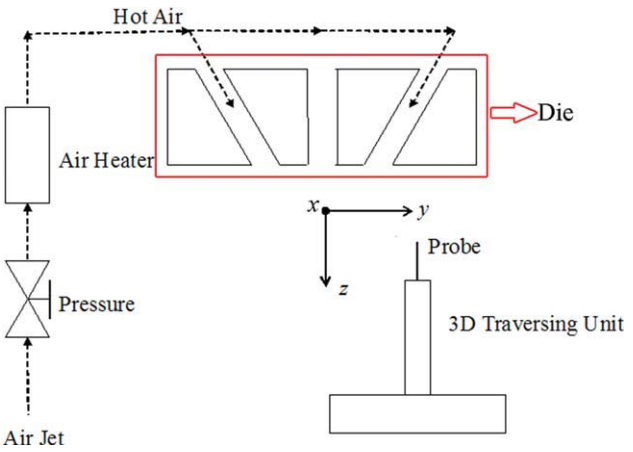

Figure 3 Experimental setup. [Color figure can be viewed in the online issue, which is available at wileyonlinelibrary.com.]

ρ is the air density, p is the air pressure, u, v, and w are the resolution of air velocity (**u**) in the x, y, and z directions, τ is the stress caused by the viscosity of air, F is gravity, T is air temperature, c_p is heat capacity, k is the convective heat-transfer coefficient, and S_T is a term of viscous dissipation.

To simulate the nonisothermal air-flow field, the air was modeled as an ideal gas with Sutherland viscosity. We used Eq. (4) to describe the relationship of ρ, temperature, and pressure:

$$P = \rho RT \tag{4}$$

where R is the molar gas constant, 287 J kg^{-1} k^{-1}.

The viscosity of an ideal gas is expressed by Sutherland's model, shown by Eq. (5):

$$\mu = \mu_0 \frac{T_0 + C}{T + C} \left(\frac{T}{T_0}\right)^{3/2} \tag{5}$$

where μ is the dynamic viscosity at temperature T, μ_0 is the reference viscosity at the reference temperature (T_0), and C is Sutherland's constant for the gaseous material.

The inlet of the calculation domain was defined as a pressure inlet with an absolute pressure of 1.3 atm. The total temperature at 403.15 K. Under the pressure inlet boundary conditions, the air jet was considered to be compressible. The outlets of the computational domain were defined as pressure outlets with atmospheric conditions. The boundary condition of symmetry was used at the center plane of the flow field. All other boundaries were assigned the default setting of being a nonslip wall. The k–ε turbulence model was adopted, and the turbulence parameters $C_{\varepsilon 1}$ and $C_{\varepsilon 2}$ were set as 1.24 and 2.05, as recommended by Krutka and Shambaugh.[7] The inlet and outlet boundary parameters were also based on their study and were set as follows: the turbulence specifications of the inlet boundary were set with an intensity of 10% and a hydraulic diameter equal to the slot width; at the pressure outlets, the turbulence intensity was 10%, and the length scale was 10 mm. It took about 40 h to complete the simulation on Dawning high-performance computer clusters with 32 quad-core 2.0-GHz Intel processors.

Experimental verification

The experiments were carried out with the single-hole melt-blowing device shown in Figure 3. The melt-blowing die had the configuration shown in Figure 2(a,b). Considering the losses of air pressure and temperature during transport in the pipe, air with a pressure of 0.2 MPa and a temperature of 533.15 K was compressed into the slots.

Air velocity and temperature below the die were measured online with a hot-wire anemometer (Dantec StreamLine CTA90C10 and Dantec StreamLine CTA 90C20, Dantec Dynamics, Skovlunde, Denmark). The anemometer probe was a metal fiber with a 5-μm diameter and a 1.2-mm length suspended between two needle-shaped prongs. The fine dimensions of the hot-wire anemometer minimized disturbance to the air flow. The hot-wire anemometer was positioned with a 3D traversing system, which permitted x, y, and z motions in 0.01-mm increments.

The coordinate system selected for the experiments is shown on Figure 3. The origin of the system is at the center of the die face. The x direction is along the major axis of the nosepiece and slots, the y direction is traverse to the major axis of the nosepiece and slots, and the z direction is directed vertically downward.

Figures 4–6 present the simulation results and the experimental data at different positions. Figure 4(a) shows the comparison of the centerline velocity predicted by computational fluid dynamics (CFD) with the measured centerline velocity, and Figure 4(b) shows the comparison of the predicted centerline temperature with the measured centerline temperature. Figure 4 indicates that the results of CFD and experiments showed considerable accord. It can be seen that the air velocity decreased rapidly near the die and gradually reached a plateau; this indicated that the velocity decay mainly occurred near the die. The temperature profile indicated that the temperature decay continued to occur with increasing distance from the die, and the decay also gradually became mild. Figure 4(b) shows that the measured and simulated temperatures below the die face at 1.5 cm were around 80°C. It is indicated that the air temperature had a severe decay from 0 to 1.5 cm. During the temperature measurement, because of the high velocity of the air jet, the probe of the hot-wire anemometer was easily broken when it was

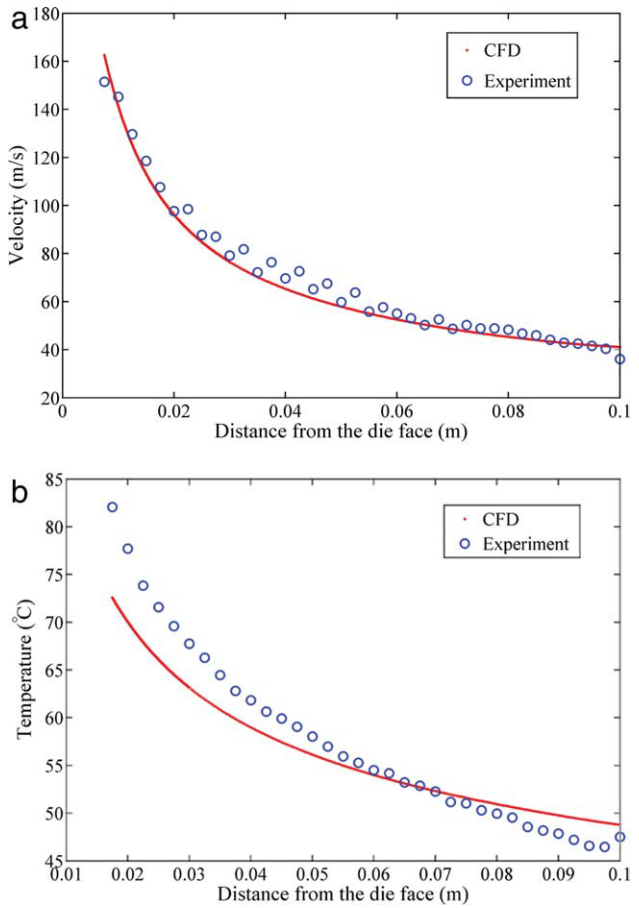

Figure 4 (a) Comparison of centerline velocity as predicted by CFD with measured centerline velocity ($x = 0$, $y = 0$). (b) Comparison of centerline temperature as predicted by CFD with measured centerline temperature ($x = 0$, $y = 0$). [Color figure can be viewed in the online issue, which is available at wileyonlinelibrary.com.]

close the die. Therefore, Figure 4(b) only shows the temperature distribution in the region from 1.5 to 10 cm. Figure 5(a,b) shows the development of velocity and the temperature profiles along the y direction at two z levels. All of the profiles in Figure 5 exhibit a single hump. As z increased from 4 to 10 cm, the velocity and temperature maximums decreased, and the profiles lost their sharp look. Figure 6(a,b) shows the velocity and temperature profiles at different x positions. Because the slot length was 6 mm [Fig. 2(a)], the position of $x = 3$ mm represented the edge of the slot, and the position of $x = 6$ was out of the slot. The profile at $x = 3$ mm was very similar with the profile at $x = 0$, whereas the profile of $x = 6$ mm had a comparable difference with the others. This indicated that the characteristics of the velocity and temperature were almost unchanged with x in the region within the slot die ($-3 \leq x \leq 3$ mm). Therefore, to save computational time, we used the results of two-dimensional (2D) simulation in the y–z plane to replace the time-consuming 3D simulation for the following optimization work. In the 2D simulation, the computation domain was the y–z symmetry plane in the 3D model, and the 2D model of the slot die is shown in Figure 7. Under the same boundary conditions of the 3D model, the 2D simulation was calculated. Figure 8(a,b) shows the centerline results comparison of the 2D and 3D simulations. The results show that it was reasonable to replace the simulation of the 3D model with that of the 2D model in the y–z symmetry plane. In the following optimization by the 2D model, the pressure inlet was set with an absolute pressure of 1.4 atm, and the total temperature was set as 593.15 K. Other boundary settings were set to be the same as those in the 3D simulation.

GA SETTINGS AND OPERATION

In the melt-blowing process, the air jet is responsible for exerting the drag force to attenuate the fiber. A higher air velocity provides a larger drag force and, therefore, results in finer fibers. However, in the flow field, the air temperature also affects fiber attenuation.

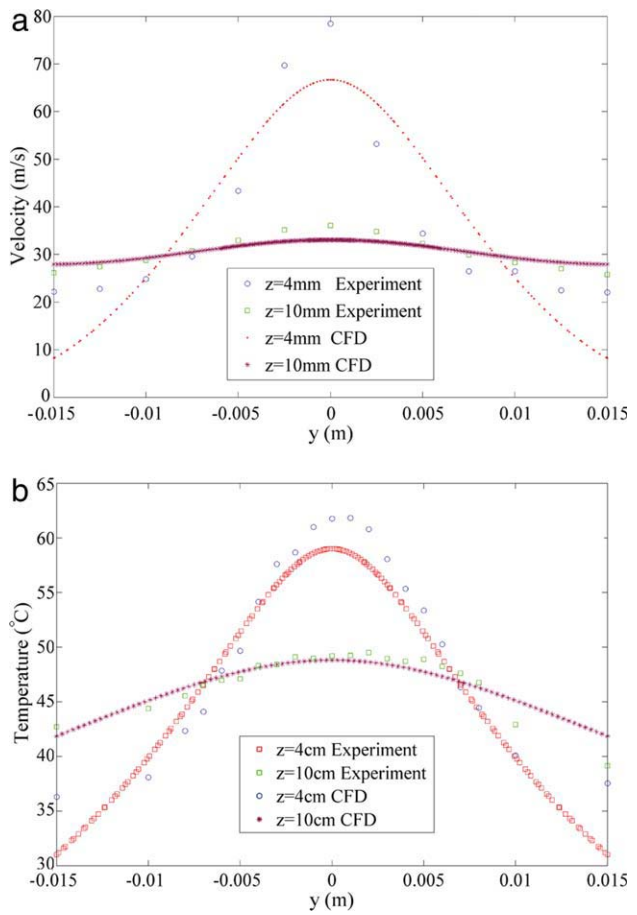

Figure 5 (a) Velocity and (b) temperature along the y direction at different z positions ($x = 0$). [Color figure can be viewed in the online issue, which is available at wileyonlinelibrary.com.]

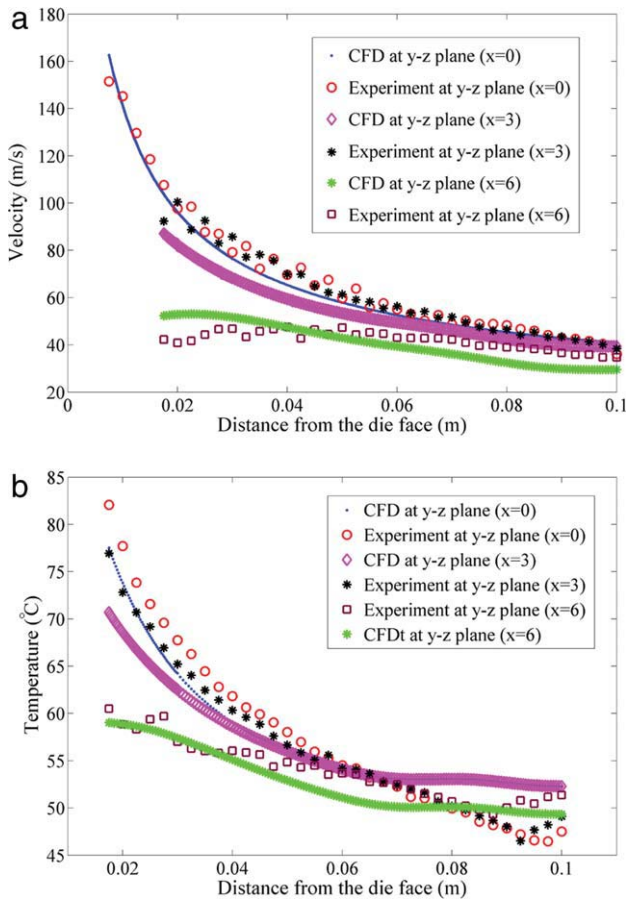

Figure 6 (a) Velocity and (b) temperature along the z direction at different x positions ($y = 0$). [Color figure can be viewed in the online issue, which is available at wileyonlinelibrary.com.]

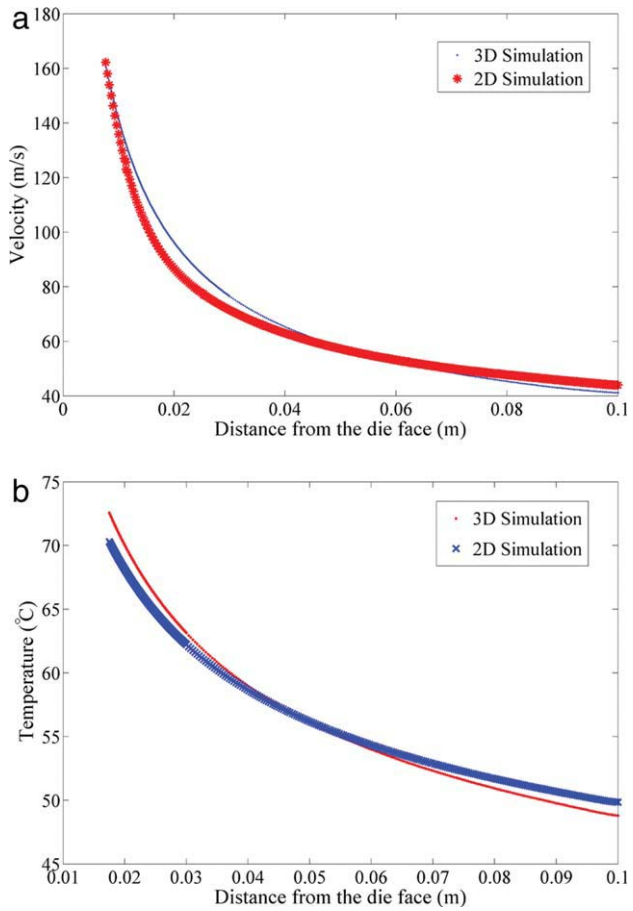

Figure 8 Flow chart of the optimizing process. [Color figure can be viewed in the online issue, which is available at wileyonlinelibrary.com.]

During the process, as soon as the molten polymer is extruded from the die, its temperature starts declining, and the solidification occurs in a position some centimeters below the die. Therefore, it is generally desirable to have the air temperature be equal to or greater than the polymer temperature. Furthermore, it is usually desirable to maintain a high air temperature along a long distance from the die. A higher air temperature will delay the solidification of the polymer and, therefore, increase the period of fiber attenuation. In a word, decreases in the air velocity and temperature both influence the melt-blowing process. In this study, we arranged a multiobjective optimization to obtain optimum air-flow field with the lowest velocity decay and temperature decay. In other words, we kept the air velocity and temperature the highest at the outlet of the calculation domain.

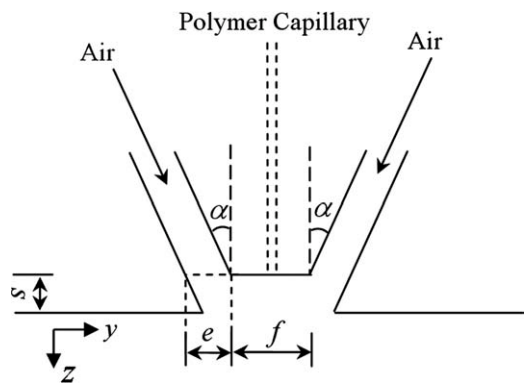

Figure 7 2D model of the slot die (i.e., the cross-sectional view of Fig. 1).

GA is a search technique used to find exact or approximate solutions to optimization and search problems. It is categorized by global search heuristics inspired by evolutionary biology, such as inheritance, mutation, selection, and crossover. Nowadays, this technique is in many research fields. For this study, GA was aimed at finding the parameter values that maximize velocity and temperature simultaneously. So it turned out to be a multiobjective optimization using genetic algorithms (MOGA). The mathematical model of this problem can be described as follows:

$$\begin{cases} \text{Minimize} & f(\mathbf{x}) = (-v_a(\mathbf{x}), -T(\mathbf{x})) \\ \text{such that} & \mathbf{x} \in X(\text{feasible region}) \end{cases} \quad (6)$$

TABLE I
Domains of the Slot Die Parameters

	Slot width (mm)	Slot angle (°)	Head width (mm)	Setback (mm)
a_i	0.1	10	0.5	0
b_i	2	80	5	1.5

where the static temperature (T) and air velocity (v_a) are obtained from numerical simulation. The variant **x** is a vector, including four decision variables: slot width (e), slot angle (α), nose-piece width (f), and setback (s; shown in Fig. 7). Each of the four parameters is set in the domain $[a_i, b_i]$. To determine the optimal values of the parameters in the feasible region (X), the domain for each parameter was much larger than that used in former studies.[7–9] Table I shows the domains of the four parameters.

The vector-evaluated genetic algorithm (VEGA) method is one of the strategies to solve MOGA. This method separates the original population into two subpopulations of equal size and distributes the optimization of the two objectives on these subpopulations. GA starts with a set of random solutions in a population; typically, a population is composed of 10–100 individuals.[13] Huang and Tang[14] successfully

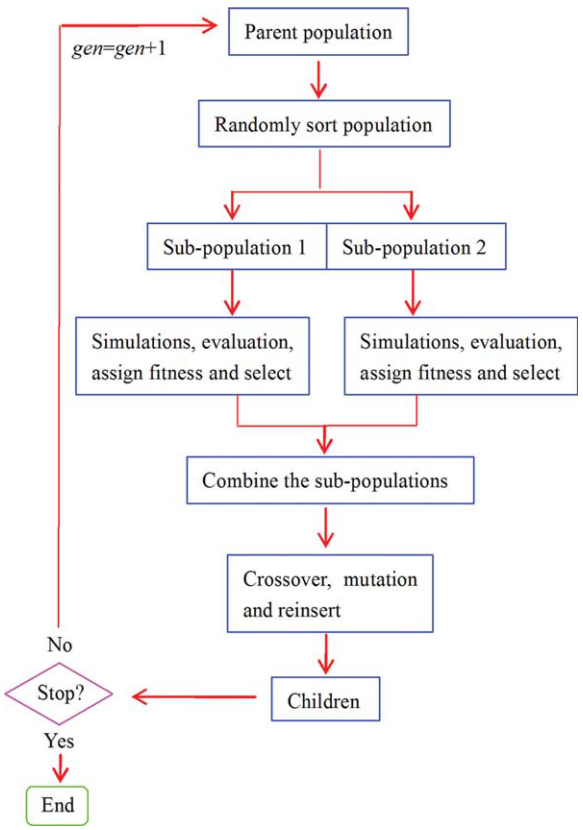

Figure 9 Values of $f(\mathbf{x})$ versus GA iterations. [Color figure can be viewed in the online issue, which is available at wileyonlinelibrary.com.]

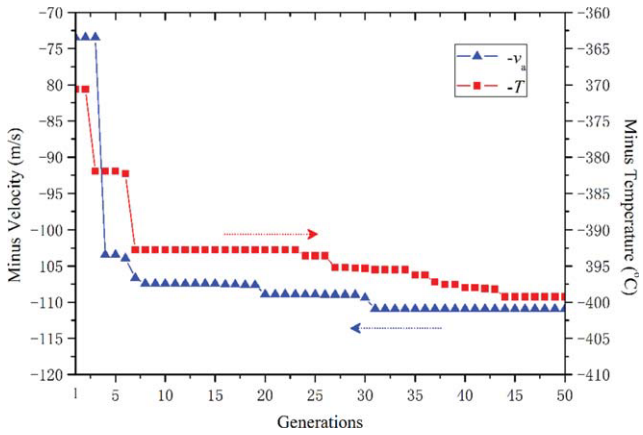

Figure 10 Variation of CV for every 10 generations. [Color figure can be viewed in the online issue, which is available at wileyonlinelibrary.com.]

optimized parameters in melt spinning by GA with a population size of 10. In this study, we set the population size at 20, and consequently, the subpopulation was 10. Each individual in the population was a chromosome. A *chromosome* is a binary string, including binary representations of all of the parameter values. The length of the binary string stands for the precision of the parameter. Considering the dimension precision of the slot die, we set the precision of each parameter at 0.001 mm; this meant that the length of chromosome was 53 bits. The search for an optimal solution to the problem was conducted over a space in a binary representation. We input parameter values of each chromosome to the simulation procedures to calculate the static temperature (T) and air velocity. The objective function $[f(\mathbf{x})]$ is used to provide a measure of how individuals have performed in the problem domain. Because the value of $f(\mathbf{x})$ is negative, which is not suitable for selection, we used a linear scaling function [Eq. (7)] to calculate the fitness of each individual:

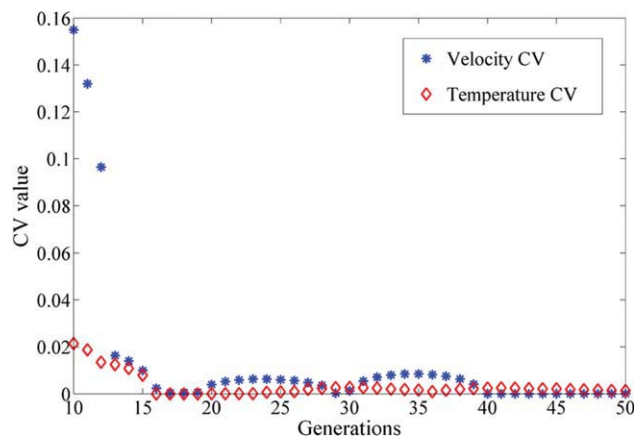

Figure 11 Centerline (a) velocity and (b) temperature of the best individual. [Color figure can be viewed in the online issue, which is available at wileyonlinelibrary.com.]

TABLE II
Optimal Geometry of the Slot Die

Slot width (mm)	Slot angle (°)	Nose-piece width (mm)	Setback (mm)
1.988	11.19	2.0147	1.393

$$F(x_i) = 2 - \mathrm{MAX} + 2(\mathrm{MAX} - 1)\frac{x_i - 1}{N_{ind} - 1} \quad (7)$$

where MAX is the upper bound of $f(\mathbf{x})$ for each generation, N_{ind} is the population size, x_i is the phenotypic value of individual i, and F is the resulting relative fitness.

The genetic operations include reproduction, crossover and mutation, and creation of the next generation. There are several methods for the process of reproduction. For this study, stochastic universal sampling was adopted. It selected a new population with respect to the probability distribution on the basis of fitness values with minimum spread and zero bias. Because GA is a method that mimics the metaphor of nature biological evolution, the rates of generation gap, crossover, and mutation all have their limits.[13] Without a loss of generosity, the generation gap is specified as 0.9, which means the fractional difference between the new and old population sizes is 0.9. The crossover and mutation rates, which determine the number of chromosomes to mate and the number of genes to mutate, respectively, are both between 0 and 1. The mutation occurs with a small probability, typically in the range 0.001–0.01.[13] In the crossover operation, several pairs of chromosomes are randomly selected, and it generates the offspring by swapping the genes from the cut point to the end of the chromosome for each pair. The mutation operation flips one of the bits of the chromosome string at a randomly selected location. For this study, the crossover rate was 0.7, and the mutation rate was 0.005. The evolution of the population repeated until the termination condition was satisfied.

RESULTS AND DISCUSSION

Figure 9 shows the flowchart of the optimizing process. The first step in VEGA is to create an initial parent population consisting of random chromosomes in the problem domain, and then, the parent population is randomly sorted into two subpopulations. These two subpopulations are input into the simulation procedure to calculate the air velocity and static temperature for each individual. According to the fitness, the genetic operations can be continued to produce the offspring. In each generation, the best individuals are left, whereas the others are discarded. As a result, the generation will be better than the former ones during the iteration. The objective value may remain stable for numbers of generations before a superior individual is found. For our study, a coefficient of variation (CV) of 10 continuous generations was used to terminate the calculation. The parameters corresponding to the minimum $-T$ and $-v_a$ were then considered as the optimum values. The commercial software MATLAB 7.0 (MathWorks, Natick, MA) provides a toolbox about GA for its users, and the VEGA was calculated in a MATLAB 7.0 environment. The CV was set to be 1.5×10^{-3}, and finally, 50 generations were carried out before the procedure was stopped. For 20 individuals in each generation, we simulated 1000 air-flow fields of the slot die. It took about 3 h to calculate a generation on the Dawning high-performance computer clusters with 32 quad-core 2.0-GHz Intel processors. The optimal individual was determined via a goal programming method, as shown in Eq. (8):

$$f(\mathbf{x}) = \left(\frac{v_a - v_a^{(0)}}{v_a^{(0)}}\right)^2 + \left(\frac{T - T^{(0)}}{T^{(0)}}\right)^2 \quad (8)$$

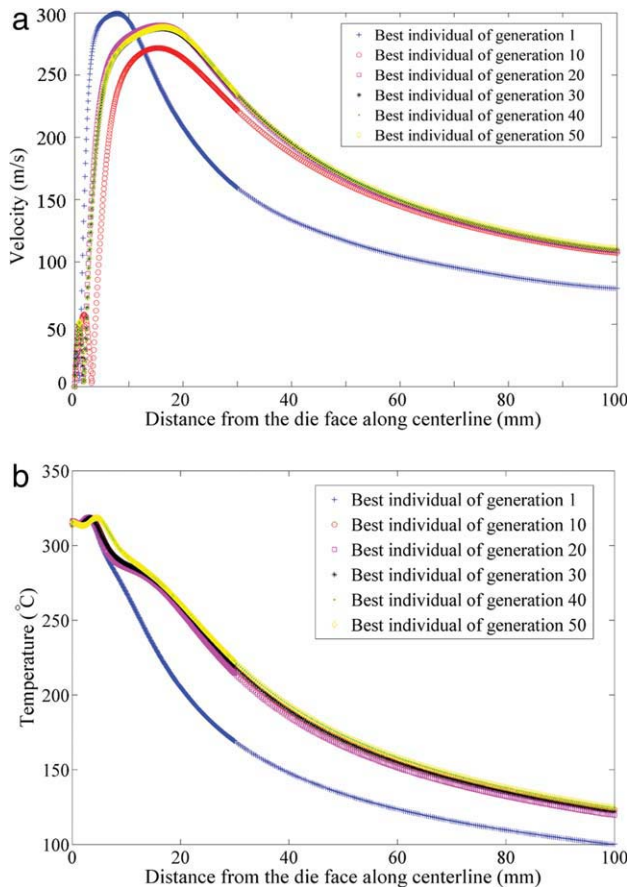

Figure 12 Centerline velocity and temperature profiles of the best individuals of generations 1, 10, 20, 30, 40, and 50. [Color figure can be viewed in the online issue, which is available at wileyonlinelibrary.com.]

where $v_a^{(0)}$ and $T^{(0)}$ are the ideal optimal values of the velocity and temperature. In this study, we chose the largest velocity and temperature along the centerline of all of the air-flow fields that we simulated as the ideal optimal values; these were 299.5 m/s and 592.585 K, respectively.

Figure 10 shows the evolution of the minimum $f(\mathbf{x}) = (-v_a, -T)$. The convergence was fast initially, and after 10 generations, the convergence slowed down and eventually led to the halting of the iteration process after 50 generations. Figure 11 shows the profile of the CV values. The final value at the 50th generation was 1.32×10^{-3}, and the optimal geometry of the slot die is shown in Table II. The optimal geometry had a maximum velocity of 109.5 m/s, with a temperature of 395.3°C. The optimal geometry also showed that the smaller slot angle and larger slot width resulted in the higher velocity and temperature.

Figure 12 gives the centerline velocity and temperature profiles of the best individuals of generations 1, 10, 20, 30, 40, and 50. We can see that the best individual of generation 50 had the lowest velocity decay and temperature decay. The simulation results of the air-flow field showed that the temperature of the air jet decreased as soon as it ejected from the die, whereas the velocity increased to its maximum and then decreased.

CONCLUSIONS

This article studied the air-flow field of the melt-blowing slot die by CFD and experiments, and the predicted and experimental results showed considerable accord. The results also show that within the slot region, a 2D simulation could replace the time-consuming 3D simulation. To optimize the air-flow field of the slot die, a systematic approach, which combined the application of numerical simulation and MOGA, was proposed. The geometry parameters, including slot width, slot angle, nose-piece width, and setback, were studied with the MOGA method. During the MOGA optimizing process, the CV was used as the terminal condition from the time-saving view. It proved that the systematic approach combining the application of numerical simulation and GA was an effective way to optimize the geometry of the melt-blowing slot die. The results show that a smaller slot angle and larger slot width resulted in lower velocity decay and temperature decay of the air-flow field.

References

1. Harpham, A. S.; Shambaugh, R. L. Ind Eng Chem Res 1996, 35, 3776.
2. Harpham, A. S.; Shambaugh, R. L. Ind Eng Chem Res 1997, 36, 3937.
3. Tate, B. D.; Shambaugh, R. L. Ind Eng Chem Res 1998, 37, 3772.
4. Bansal, V.; Shambaugh, R. L. Ind Eng Chem Res 1998, 37, 1799.
5. Tate, B. D.; Shambaugh, R. L. Ind Eng Chem Res 2004, 43, 5405
6. Bresee, R. R.; Ko, W. C. Int Nonwovens J 2003, 12, 21.
7. Krutka, H. M.; Shambaugh, R. L. Ind Eng Chem Res 2002, 41, 5125.
8. Moore, E. M.; Shambaugh, R. L. J Appl Polym Sci 2004, 94, 909.
9. Krutka, H. M.; Shambaugh, R. L.; Papavassiliou, D. V. Ind Eng Chem Res 2005, 44, 8922.
10. Krutka, H. M.; Shambaugh, R. L.; Papavassiliou, D. V. Ind Eng Chem Res 2006, 45, 5098.
11. Sun, Y. F.; Wang, X. H. J Appl Polym Sci 2009, 115, 1540.
12. Karr, C. L. Proc 4th ICGA 1991, 450.
13. Goldberg, D. E. Genetic Algorithms in Search, Optimization and Machine Learning; Addison Wesley: Reading, MA, 1989.
14. Huang, C. C.; Tang, T. T. Int J Adv Manufacturing Technol 2006, 27, 1113.